

Vectorial mechanism of nonlinearity enhancement in rubidium vapor

Mecanismo vectorial para mejorar la no linealidad en vapor de rubidio

Nikolai Korneev*, Chrystian Gutiérrez Parra*

ABSTRACT

We report the calculations of vectorial nonlinear properties of rubidium vapor for ^{87}Rb D_2 transition at moderate intensities. Different from Kerr nonlinearity, optimal intensity exists here, which depends on beam geometry. For intensities close to the optimal, the vectorial mechanism is much more efficient than a scalar one.

RESUMEN

Presentamos los cálculos de las propiedades no lineales vectoriales del vapor de rubidio para la transición ^{87}Rb D_2 a intensidades moderadas. Diferente de la no linealidad Kerr, existe aquí una intensidad óptima, la cual depende de la geometría del haz. Para intensidades próximas a la óptima, el mecanismo vectorial es mucho más eficiente que un mecanismo escalar.

INTRODUCTION

Rubidium vapor for laser frequency, close to the transition frequency, is well known as nonlinear optical medium (Zerom & Boyd, 2009). Strong self-action effects, including pattern formation, were observed in it with high power focused beams. For theoretical description, the nonlinearity is usually taken in a simple scalar Kerr form. For laser frequency far enough from the transition, the Kerr coefficient can be obtained from the two-level model as a result of saturation. For multilevel atoms and strong laser fields, however, the effects of atomic coherence can become important. In this case the level populations alone are not sufficient to explain the medium response to light, and it is necessary to consider phase information of atomic state or a density matrix. The coherent effects actively studied actually include among others electromagnetically induced transparency (Fleischhauer, Imamoglu & Marangos, 2005), dark states (Arimondo, 1996), and nonlinear magneto-optical effects (Budker, Gawlik, Kimball, Rochester, Yashchuk & Weis, 2002). Polarized light is important in creating atomic coherence, and thus nonlinearities can be strongly modified (enhanced or diminished) by manipulations with light polarization. Though general mechanisms are quite well understood, an adequate theoretical description for experimentally important intensities and detunings is difficult because of the multilevel structure of rubidium transition.

We present results of nonlinearity calculation, based on the direct solution for density matrix evolution in the ^{87}Rb D_2 line. The solution procedure is similar to the one reported in Korneev & Benavides (2008, 2009). We can see that there is an optimal light intensity, for which the nonlinearity is the highest, and this optimal intensity depends on time of flight (beam diameter), and an elliptic polarization combined with weak longitudinal magnetic field (Korneev, 2011). The nonlinearity has nontrivial spectral dependences as well.

Recibido: 13 de Noviembre del 2012
Aceptado: 7 de junio del 2013

Keywords:

Rubidium; Kerr effect; cross-phase modulation.

Palabras clave:

Rubidio; efecto Kerr; modulación de fase cruzada.

*National Institute for Astrophysics, Optics and Electronics (INAOE). Apdo. postal 51 and 216, Tonantzintla, Puebla, México. 72000. E-mail: korneev@inaoep.mx; chrysg@inaoep.mx

Theoretical model

We work with a basis of circular polarization amplitudes σ_1, σ_2 and we use the equivalent Rabi frequencies Ω_1, Ω_2 . The two components of nonlinear medium polarization can be written, when we take the account into the rotational symmetry of problem, for longitudinal magnetic field, in the form ($i = 1, 2$):

$$P_i = F_i(|\sigma_1|, |\sigma_2|)\sigma_i = F_i(\Omega_1, \Omega_2)\sigma_i. \quad (1)$$

The physical situation that we consider is an interaction of a strong pump beam with a weak probe. The probe slightly changes the pump intensity and/or polarization state. The nonlinear interaction is given by a 2 by 2 matrix, estimated for the pump parameters and proportional to:

$$\begin{pmatrix} \frac{\partial F_1}{\partial \Omega_1} \Omega_1 & \frac{\partial F_1}{\partial \Omega_2} \Omega_2 \\ \frac{\partial F_2}{\partial \Omega_1} \Omega_1 & \frac{\partial F_2}{\partial \Omega_2} \Omega_2 \end{pmatrix}, \quad (2)$$

Such matrix appears when we consider the first approximation of the three-wave mixing including the strong pump and a pair of weak symmetric side orders. The matrix eigenvectors give the proper polarizations of side beams, which are maintained along propagation, and corresponding eigenvalues give equivalent Kerr constants for a polarization in question.

Mathematically, the problem for proper polarization is then reduced to a scalar Kerr interaction, which gives, well-known, modulation instability type solution for positive eigenvalues.

Solving the eigenvalue problem for the matrix equation (2) is trivial for linear polarization of a pump ($\Omega_1 = \Omega_2$) and zero magnetic field, thus the matrix is symmetric, and there are two proper polarizations of probe beam. Their eigenvalues are:

$$\eta_{\pm} = \frac{F_1}{\partial \Omega_1} \Omega_1 \pm \frac{\partial F_1}{\partial \Omega_2} \Omega_2, \text{ for } \Omega_1 = \Omega_2 = \Omega. \quad (3)$$

The η_+ coefficient describes the self-phase modulation, and it gives the usual scalar Kerr nonlinearity. The η_- coefficient determines an interaction of a linearly polarized pump beam with an orthogonally polarized signal beam. Also, it gives the difference of refractive index for two circular components in response to the

polarization ellipticity. The ellipticity coefficient ε is determined as follows:

$$\tan \varepsilon = \frac{\sigma_2 - \sigma_1}{\sigma_2 + \sigma_1}. \quad (4)$$

Following, reference (Agarwal, 1974), to calculate medium polarizations we use the master equation for density matrix ρ evolution:

$$\frac{\partial \rho}{\partial t} = (i/\hbar)[\rho, H] + \sum_{q=-1,0,1} C_q \rho C_q^+ - \frac{1}{2}(C_q^+ C_q \rho + \rho C_q^+ C_q). \quad (5)$$

where H is the Hamiltonian of an atom, and C_q, C_q^+ are lowering and raising atomic operators:

$$\begin{aligned} C_q^+ \left| F_g, m_{F_g} \right\rangle &= \Gamma^{1/2} (1, F_g, q, m_{F_g}; F_e, m_{F_e} \\ &= m_{F_g} + q) \left| F_e, m_{F_e} = m_{F_g} + q \right\rangle, \\ C_q^+ \left| F_e, m_{F_e} \right\rangle &= 0, \\ C_q &= (C_q^+)^*. \end{aligned} \quad (6)$$

with a decay rate Γ , and Clebsch-Gordan coefficients for coupling ground, and excited, state sublevels.

The evolution given by the equation (5) is calculated numerically for a characteristic time of flight τ , using a fast special algorithm described in reference (Korneev & Benavides, 2008, 2009). The derivatives in equation (2) are calculated numerically using close values of Rabi frequencies for a necessary number of detunings. After this, the convolution with Doppler lineshape is performed, which gives the approximation to experimentally observable spectra.

RESULTS OF NUMERICAL MODELLING

We first concentrate on the case of zero magnetic field and linear pump polarization in $F_g = 2$ ^{87}Rb D_2 line (780.24 nm). The interest in this particular transition is due to two reasons. First, in this line the highest three-wave mixing gain is observed for intensities in the 10 mW - 30 mW range of laser power, and second, calculations in ^{87}Rb are somewhat faster, than in ^{85}Rb because of smaller sublevel number for this isotope.

The spectra of cross-phase modulation coefficient prove to be strongly dependent on the time of flight and light intensity (figures 1, 2). However, smaller intensities and bigger flight times (wider beams) give somewhat higher maximal nonlinearity values in a positive spike (figure 1).

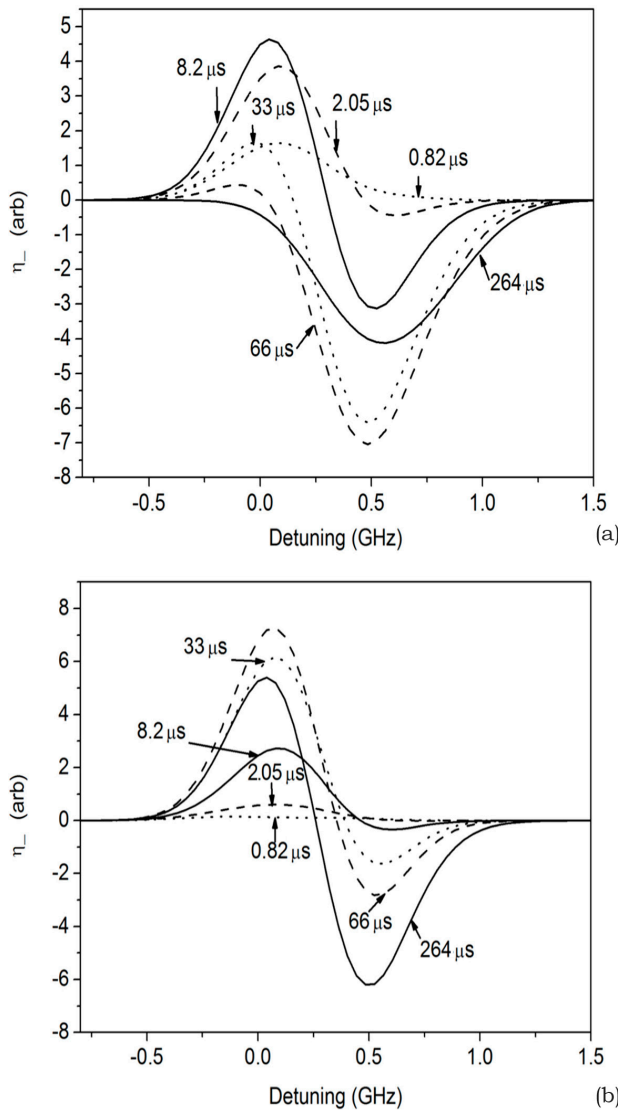


Figure 1. Cross-phase modulation spectra in $F_g = 2$ line for two intensities (a) 8.54 mW/mm^2 and (b) 0.53 mW/mm^2 both with different times of flight. The zero frequency corresponds to $F_g = 2$, $F_e = 2$ transition. Source: Authors own elaboration.

The action of making intensity higher with a fixed time of flight is similar to making bigger the time of flight with a fixed intensity (figure 2). The nonlinearity can be further enhanced with a combination of a weak magnetic field and elliptic polarization of a pump (either of these factors separately diminishes nonlinearity strength).

The relative importance of different nonlinear processes near the lower optimum intensity is shown

in figure 3(a). It is seen, that for moderate intensity one can expect approximately an order of magnitude nonlinearity strength growth if vectorial nonlinearity is used instead of a traditional Kerr one. The figure 3(b) shows that the nonlinearity is increased when the magnetic field is applied, until it reaches a maximum, and it decreases for still higher fields. When we have a small ellipticity ($\epsilon = -0.061$) it reaches a maximum with a small magnetic field ($B = 0.51 \text{ G}$). For a given time of flight and intensity there is only one combination of ϵ and B which gives an optimal nonlinearity.

Experiment

In the experiments we used 75 mm long natural rubidium cell placed inside two protective shells made of μ -metal. The electric heater was placed between the two shells. A longitudinal magnetic field is produced with a solenoid. We were using a 50 mW tuneable external cavity diode laser. The setup is described in reference (Korneev & Gutiérrez-Parra, 2012). The results for one beam diameters are presented in figure 4. The set of curves was obtained by loosely focusing a beam with big focal length lens onto a cell, which produced a gaussian beam radius of $0.17 \text{ mm} \pm 0.02 \text{ mm}$. Also a 0.5 mm diameter diaphragm was placed in a far field before the detecting beamsplitter to measure the rotation in a beam centre. The behaviour of these curves is generally consistent with a theoretical analysis in figures 1, 2. In particular, the optimal light intensity is clearly seen for both beam widths.

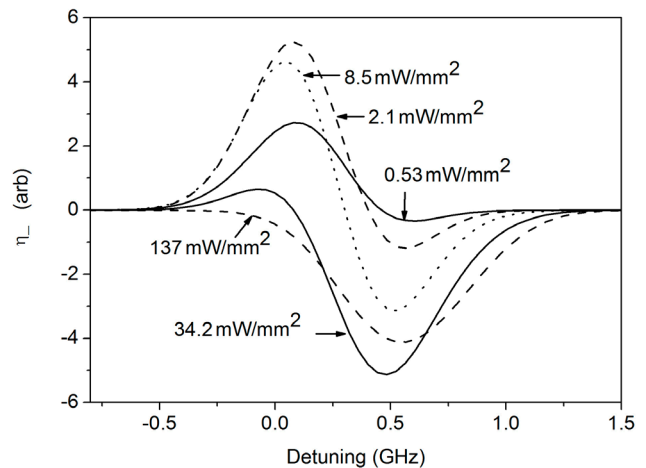


Figure 2. Cross-phase modulation spectra in $F_g = 2$ line for time of flight $8.2 \mu\text{s}$ and different intensities. Source: Authors own elaboration.

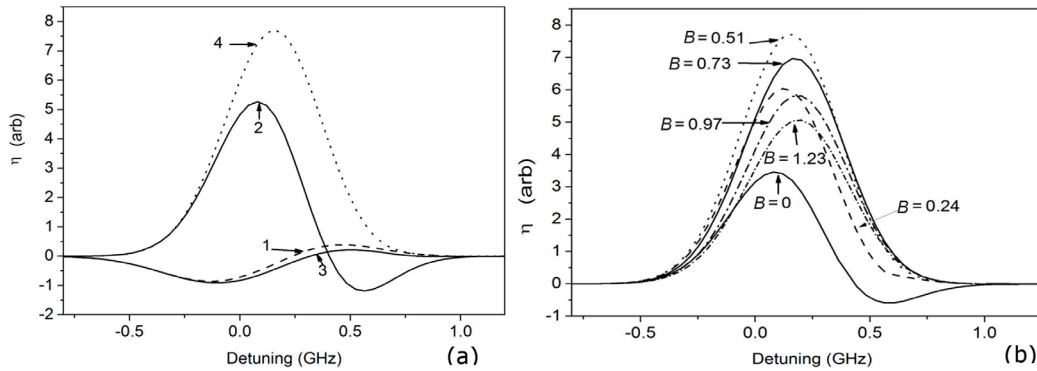


Figure 3. (a) Curve 1 – zero magnetic field, η_1 ; curve 2 – zero magnetic field, η_2 with ellipticity $\varepsilon = 0$; curves 3 and 4 – two eigenvalues for ellipticity $\varepsilon = -0.061$, and magnetic field $B = 0.51$ G. Time of flight $8.2 \mu\text{s}$, intensity 2.1 mW/mm^2 . (b) Eigenvalues for ellipticity $\varepsilon = -0.061$ and different magnetic fields. Time of flight $8.2 \mu\text{s}$, intensity 2.1 mW/mm^2 .

Source: Authors own elaboration.

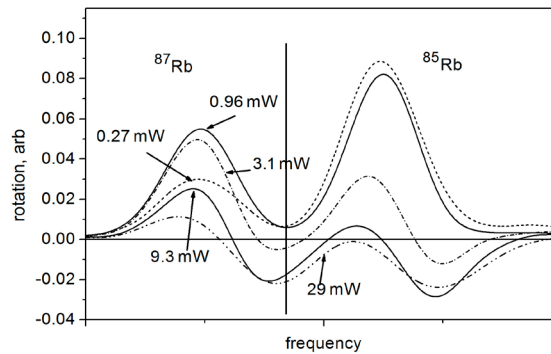


Figure 4. Self-rotation signal for different beam powers. The gaussian beam radius is $r = 0.17 \text{ mm} \pm 0.02 \text{ mm}$. The behaviour in $^{87}\text{Rb } F_g = 2$ transition (left spike) qualitatively corresponds to the theoretical curves in figure 2.

Source: Authors own elaboration.

CONCLUSIONS

The numerical solution of the full density matrix evolution equation permits a good estimation of factors affecting vectorial nonlinearity strength in rubidium vapour, and it provides useful guidelines for experiments. For obtaining strong nonlinear effects at moderate intensities, it is necessary to adjust polarization state, light intensity, magnetic field and beam geometry. The results show that the vectorial interaction for intensities typical of tuneable semiconductor lasers do not demonstrate a simple Kerr character. More results and analysis are shown in reference (Korneev & Gutiérrez-Parra, 2012).

ACKNOWLEDGEMENT

We acknowledge the *Secretaría de Educación Pública-Subsecretaría de Educación Superior-Dirección General de Educación Superior Universitaria* project 2012-01-21-002-205 and *Consejo Nacional de Ciencia y Tec-*

nología (Conacyt) project 00000000189688 for supporting the LAOP Workshop 2012, where this work was presented. This work was done within the Conacyt project CB/156891.

REFERENCES

- Agarwal, G. S. (1974). *Quantum statistical theories of spontaneous emission and their relation to other approaches*. USA: Springer Verlag.
- Arimondo, E. (1996). Coherent population trapping in laser spectroscopy. *Progress in Optics*, 35, 257-354.
- Budker, D., Gawlik, W., Kimball, D. F., Rochester, S. M., Yashchuk, V. V. & Weis, A. (2002). Resonant nonlinear magneto-optical effects in atoms. *Reviews of Modern Physics*, 74(2), 1153-1201.
- Fleischhauer, M., Imamoglu, A. & Marangos, J. P. (2005). Electromagnetically induced transparency: Optics in coherent media. *Reviews of Modern Physics*, 77(2), 633-673.
- Korneev, N. (2011). Nonlinearity enhancement in rubidium vapour with vectorial mechanism. *Journal of the Optical Society of America B*, 29(9), 2588- 2594.

- Korneev, N. & Benavides, O. (2008). Mechanisms of holographic recording in rubidium vapour close to resonance. *Journal of Optical Society of America B*, 25(11), 1899-1906.
- Korneev, N. & Benavides, O. (2009). Direct multi-level density matrix calculation of nonlinear optical rotation spectra in rubidium vapour. *Journal of Modern Optics*, 56(10), 1194-1198.
- Korneev, N. & Gutiérrez-Parra, C. (2012). Vectorial mechanism of nonlinearity enhancement in rubidium vapour. *Journal of Optical Society of America B*, 29(9), 2588-2594.
- Zerom, P. & Boyd, R. W. (2009). Self-focusing, conical emission, and other self-action effects in atomic vapors'. In R. W. Boyd, S. G. Lukishova & Y. R. Shen (Ed.), *Self-focusing: Past and Present. Fundamentals and Prospects* (pp. 231-251). USA: Springer.